Original Article
Propofol accelerates lung cancer cells apoptosis through regulation of Rno-miR-665 and BCLXL expression

Jie Bai*, Yi Li*, Yingbin Wang, Shenghui Huang, Shuangyin Zhang, Yufang Hua

*Department of Anesthesiology, The Second Hospital of Lanzhou University, Lanzhou, Gansu Province, P. R. China. *Equal contributors.*

Abstract: Background: Non-small-cell lung cancer is the leading cause of cancer-related mortality in human worldwide. Propofol is widely used in general anesthesia and sedation, which is also well-known for its anti-tumor function in many cancer cells. Methods: Cck8 assay was used for cell proliferation test; Flow cytometer, TUNEL assay and caspase-3 activity analysis were used for cell apoptosis. After transfected with rno-miR-665 mimics or inhibitor in A549 cells, the functions of proliferation and apoptosis was investigated. Quantitative polymerase chain reaction analysis and western blot were performed to detect the expression of related proteins in A549 cells. The target gene of rno-miR-665 was determined by luciferase assay and Western blot. Results: Propofol inhibited A549 cell proliferation and induced cell apoptosis significantly *in vitro*. Introduction of rno-miR-665 mimics apparently suppressed the proliferation and induced apoptosis of A549 cells, while transfection with rno-miR-665 inhibitor in A549 cells contributed to propofol not alter cell proliferation and apoptosis. Moreover, luciferase reporter assay identified the 3'-UTR of bcl-xl mRNA contained a complementary sequence for rno-miR-665. Bcl-xl was a direct target of rno-miR-665. Conclusion: Propofol inhibits proliferation and induces apoptosis of A549 cells through, at least partly, regulation of rno-miR-665. Our study provided a better understanding of propofol function in NSCLC cells.

Keywords: Non-small-cell lung cancer, MicroRNAs, propofol, bcl-xl, proliferation, apoptosis

Introduction

NSCLC, non-small-cell lung cancer accounts for 80%-85% of lung cancer, which is the leading cause of cancer-related mortality in human worldwide [1-3]. Due to implementation of tobacco control and advances in multidisciplinary treatments, both incidence and mortality have slowly declined. However, majority of lung cancer patients diagnosed at advanced-stage, in addition to high relapse rate, the 5-year survival rate of NSCLC is only 13% [4].

Propofol, a rapid onset and comfort recovery intravenous anesthetic, is widely used in general anesthesia and sedation. Propofol is also well-known for its anti-inflammatory, anti-oxidant and induce apoptosis. These effects have been demonstrated in accumulating clinical evidences [5-7]. Moreover, the fact that propofol total intravenous anesthesia for cancer surgery decreases the risk of recurrence during the initial years of follow-up [8-10], indicates that propofol has the effect to inhibit cancer cells released into the circulation in the perioperative period. Propofol functions in cancer cells involve various mechanisms. Biki B et al suggested that propofol induced apparent cell death in the hESC-derived neurons by regulation of microRNAs expression [11], and Sun et al presented that propofol-induced disturbances in astroglia development might be related with rnomiR-665 [12].

MicroRNAs (miRNAs) are endogenous, non-coding RNA molecules that mediate target sequence-specific mRNA degradation [13] or repression of mRNA translation [14] to regulate nearly every cellular process. The role for miRNAs in the carcinogenesis, development and progression of NSCLC has been well established [15-17]. Recently, Sun et al found that

rno-miR-665 was significantly regulated by propofol in vitro, and we suspect that whether such effect found in NSCLC.

Given the above research, we hypothesized that regulation of the expression of rno-miR-665 might be involved in the mechanism of inducing apoptosis of propofol in NSCLC.

Materials and methods

Cell culture and reagent

Human NSCLC cell A549 was purchased from Shanghai Institutes for Biological Sciences and maintained in RPMI 1640 medium (Gibco) supplemented with 10% fetal bovine serum (Sigma Aldrich, St. Louis) in a 5% CO_2 incubator at 37°C. A549 cells medium also involved 100 IU/ml penicillin and 100 μg/ml streptomycin (Solarbio, China). Cells were harvested at 80% confluence.

Pure propofol (2,6-diisopropylphenol) was obtained from Beyotime. A stock solution (40 mg/mL) of propofol was prepared in RPMI 1640 medium and stored at -20°C.

Cell proliferation detection

Cell proliferation of A549 was assessed by cell counting kit-8 (CCK-8) assay (Beyotime) which is based on bioreduction of 2-(2-methoxy-4-nitrophenyl)-3-(4-nitrophenyl)-5-(2,4-disulfophenyl)-2H tetrazolium sodium (WST-8) to measure cell proliferation viability. According to the manufacturer's instructions, cells were seeded into 96-well plates at 8,000 cells per well and allowed to adhere overnight. The cells were then co-incubated with propofol at various concentrations (0 μM, 1 μM, 5 μM, or 10 μM) for 48 h before 10 μL CCK-8 assay reagent was added into each well. After incubation at 37°C for 2 h, optical density units of absorbance at 450 nm were measured. The samples consisted of wells with treated cells, the blanks consisted of wells without cells, and the controls consisted of wells with untreated cells.

Flow cytometer for apoptosis assay

A549 cell apoptosis was analyzed by the Annexin V-APC Apoptosis Detection Kit (KeyGEN Biotech, Nanjing, China) and evaluated with a flow cytometry analyzer (BD Biosciences, San Jose, CA). Cells (10^6/well) were treated with 10 μM propofol for 24 h, then washed twice with cold phosphate-buffered saline solution (PBS) to remove floating cells and harvested left cell for apoptosis analysis. Data were analyzed by BD Accuri C6 software.

Terminal deoxynucleotidyl transferase (TdT) dUTP nick-end labeling assay

Apoptotic cells also detected by terminal deoxynucleotidyl transferase (TdT) dUTP nick-end labeling (TUNEL) (Roche, Shanghai, China) assay for that late stages of apoptosis undergo extensive DNA degradation [18]. Cells were fixed with 4% paraformaldehyde and 0.2% Triton X-100, and then incubated with in situ cell death detection kit (Roche, Shanghai, China) at 37°C for 1 h. After that, the samples were mounted in mounting media containing DAPI. Fluorescent images were captured and the total numbers of DAPI positive cells or TUNEL positive cells were counted from at least five images.

Caspase-3 activity analysis for cell apoptosis

Caspase-3 colorimetric activity assay kit (Beyotime, Shanghai, China) was used for detecting caspase-3 activity of A549 cells. In brief, cells treated by 10 μM propofol were washed twice with PBS and lysed with the cell lysis buffer included in the kit to collect proteins. Equal amounts of protein were incubated with caspase-3 substrate (Ac-DEVD-AMC) at 37°C for 2 h. Caspase-3 activity was determined by measuring the absorbance at 405 nm.

Plasmid transfection

A549 cells were seeded into 12-well plates and kept in an incubator at 37°C overnight. Subconfluent cells were transfected with pG-CMV/EGFP plasmids containing rno-miR-665 mimic, rno-miR-665 inhibitor or empty vector (negative control [NC]) using Lipofectamine 2000 (Invitrogen-Life Technologies, CA) (DNA/Lipofectamine 2000=1/2.5), all the plasmids were synthesized by GenePharma (Shanghai, China). Cells were incubated in complete DMEM with blasticidin (12 μg/mL) (Sigma, Shanghai, China) or G418 (500 mg/ml) (Sigma, Shanghai, China) for 15 days. We verified clones from stable transfection expression of cell lines using quantitative polymerase chain reaction analy-
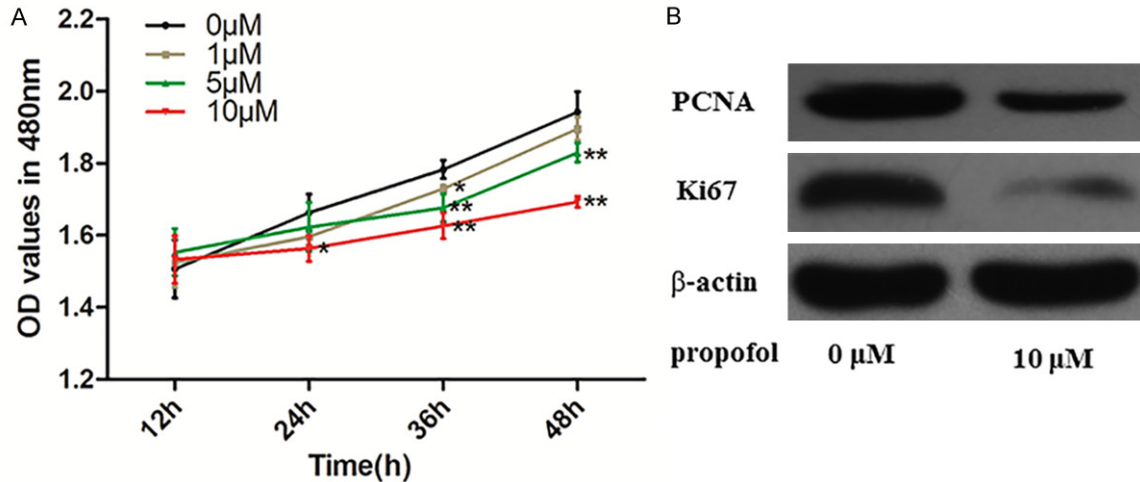
Figure 1. Propofol inhibits A549 cell proliferation. A: Different concentration of propofol (1, 5 or 10 μM) treated A549 cells for 48 h resulted in dose- and time- dependent cell proliferation inhibition compared to the control; B: Propofol decreased the protein expression levels of PCNA and ki-67 in A549 cells. *P<0.05 **P<0.01 vs. control.

sis (qPCR) and Western blot, and then kept the successful clones for further experiments.

Isolation of RNA and quantitative polymerase chain reaction analysis

Total RNA from A549 cells was extracted by TRIzol (Invitrogen, Shanghai, China) following the manufacturer's protocols, miRNA-specific RT primers (RiboBio, Guangzhou, China) for rno-miR-665 and random primer (TaKaRa, Dalian, China) for bcl-xl. Reverse-transcribed cDNA was measured by quantitative polymerase chain reaction (qPCR) using SYBR Green PCR Kit (QIAGEN, Shanghai, China) under the following conditions: denaturation at 95°C for 5 min, then 40 cycles of denaturation at 95°C for 10 sec and annealing and extension at 60°C for 30 sec in an Applied Biosystems 7500 Fast Sequence Detection System. The relative miRNA and mRNA expression levels were normalized by U6 and β-actin, respectively. Relative expression and fold differences were determined by comparing normalized expression levels between groups (ΔΔCT) using the $2^{-\Delta\Delta CT}$ method.

The reverse transcription primer rno-miR-665: 5'-GTCGTATCCAGTGCAGGGTCCGAGGTATTCGC-ACTGGATACGACTAAGGG-3' The qPCR primers: rno-miR-665: 5'-GGTGAACCAGGAGGCTGAGG-3' (forward), 5'-CAGTGCAGGGTCCGAGGTAT-3' (reverse); BCLXL: 5'-ATCAGAAACGCCAGCGAA-GA-3' (forward), 5'-TCAGATACCACAAAGCACCA-3'

(reverse); β-actin: 5'-GGAGATTACTGCCCTGGC-TCCTAGC-3' (forward), 5'-GGCCGGACTCATCGT-ACTCCTGCTT-3' (reverse).

Western blotting

Treated cells were washed and lysed to collect proteins from the supernatant fraction. Protein concentration was measured by bicinchoninic acid protein assay kit (Beyotime, Hangzhou, China). All proteins were separated by 10% sodium dodecyl sulfate-denatured polyacrylamide gel electrophoresis and subsequently transferred to nitrocellulose membrane (Bio-Rad), After blocking with 5% nonfat dried milk and incubation of membranes at 4°C overnight with primary antibody (1:1000 dilution), the membranes were then reacted with horseradish peroxidase-conjugated secondary antibody (1:2000 dilution; both, Santa Cruz Biotechnology) at room temperature for 1 h. The blots were then incubated with enhanced chemiluminescence solution for 1 min. Final signals were detected by the ChemiDoc XRS + Chemiluminescence imaging system (Bio-Rad, Hercules, CA) and specific bands were visualized with a UVP Gel imaging system and analyzed by an Image-Pro Plus 6.0 system.

Luminescent reporter gene transfection and luciferase assays

The putative rno-miR-665 binding sites in the bcl-xl 3' UTR was predicted by using the
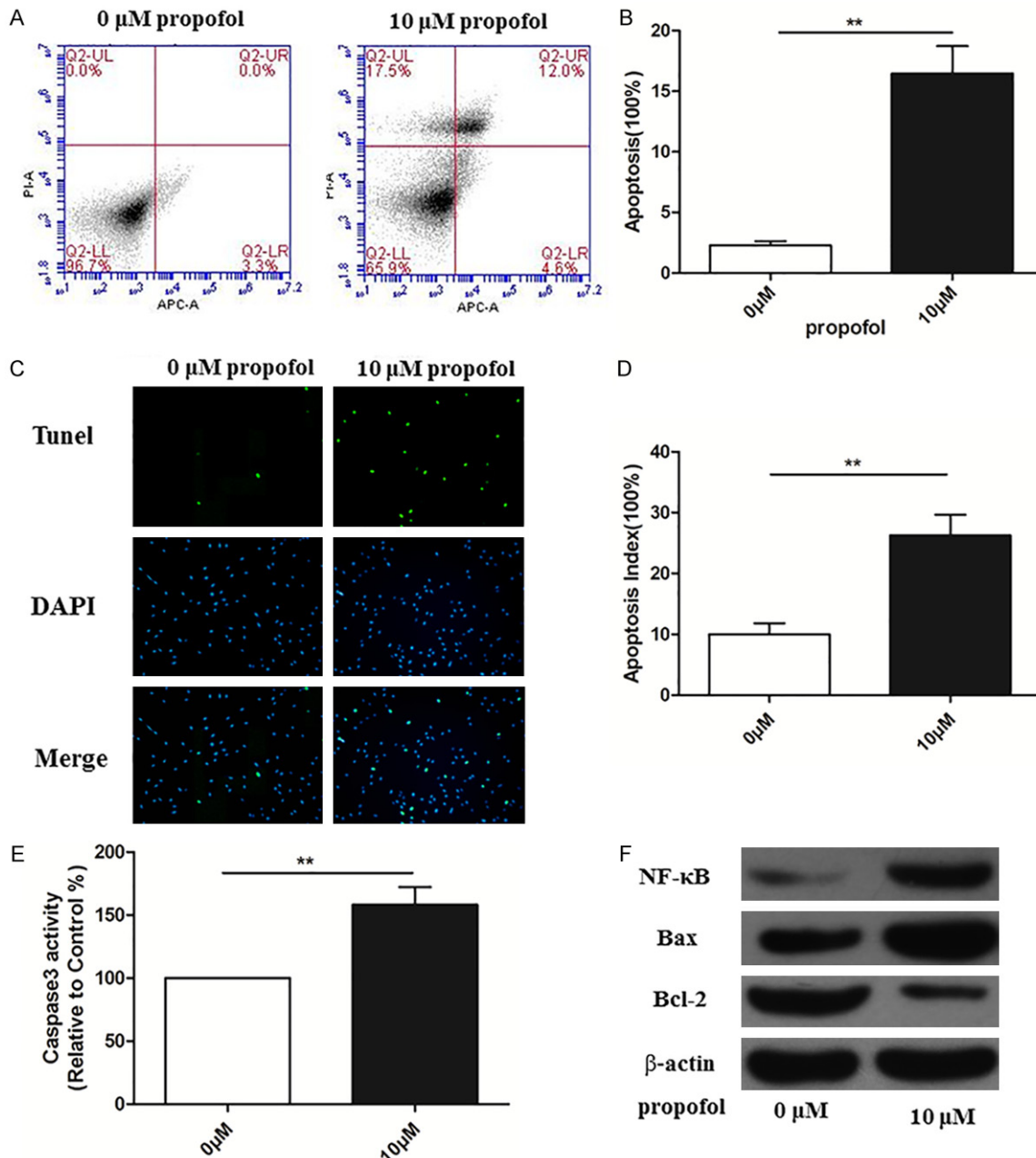
Figure 2. Propofol induces A549 cells apoptosis. A, B: 10 µM propofol treatment for 24 h increased both early and late apoptotic cell populations compared with the control; C, D: Percentage of TUNEL positive cells in A549 cells treated with propofol significantly increased compared with control; E: Caspase-3 activity was increased dramatically after treatment by propofol; F: Protein expression levels of NF-κB, bax and bcl-2 in A549 cells were all in accordance with the above. **P<0.01 vs. control.

TargetScan and miRanda database. For the luciferase activity assay, the mRNA 3'-UTR sequences of the bcl-xl (WT) was PCR amplified and inserted downstream of the Renilla luciferase gene in a Renilla/firefly luciferase reporter plasmid, psiCHECK-2 (GenePharma, Shanghai, China). The forward primer sequences for the mRNA 3'-UTR of bcl-xl was 5'-ATCAGAAACG-CCAGCGAAGA-3' and reverse primer sequences was 5'-TCAGATACCACAAAGCACCA-3'. Bcl-xl mRNA 3'-UTR contained sequences with mutations (MUT) in the putative binding sites of rno-miR-665 was chemically synthesized by GenePharma. A549 cells were transfected with WT or MUT constructed reporter plasmids and rno-miR-665 mimics or mimics control by using
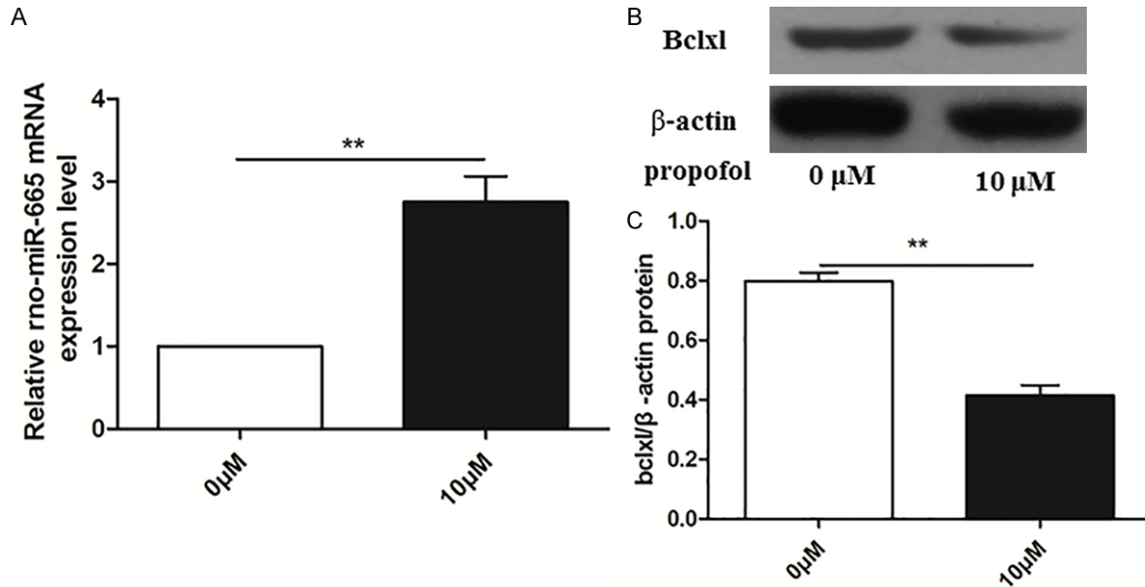
Figure 3. Propofol increases rno-miR-665 and decreases bcl-xl expression in A549 cell. A: Rno-miR-665 elevated in A549 cells after 10 µM propofol treatment for 24 h; B, C: Propofol significantly decreased the expression of bcl-xl in A549 cells. **P<0.01 vs. control.

Lipofectamine 2000. Incubated at 37°C for 48 h post-transfection, both firefly and Renilla luciferase activities were measured by a dual luciferase reporter assay (Promega, Madison, WI) in an automatic microplate reader (Thermo Scientific, Waltham, MA).

Statistical analysis

Statistical analysis was conducted using SPSS software version 18.0 (SPSS Inc., Chicago, IL, USA) and GraphPad Prism 5 (La Jolla, CA) software packages. All results are expressed as means ± standard deviation (SD), Each sample was run in triplicate. Comparisons between groups were analyzed by analysis of variance or 2-tailed Student t-test. A *P*-value <0.05 was considered statistically significant.

Results

Propofol inhibits A549 cell proliferation

The effect of propofol on proliferation of A549 cells was detected by cck8 assay. As shown in **Figure 1A**, treatment of A549 cells with propofol (1, 5 or 10 µM) for 48 h resulted in dose- and time- dependent cell proliferation inhibition compared to the control (all panels, P<0.05-0.01). We also found that treatment of propofol decreased the protein expression levels of PCNA and ki-67 in A549 cells (**Figure**

1B), which agreed with the results of the cck8 assay.

Propofol induces A549 cells apoptosis

10 µM propofol treatment for 24 h increased both early and late apoptotic cell populations compared with the control (P<0.01) (**Figure 2A, 2B**). Apoptosis was also measured using TUNEL assay, propofol could significantly increased percentage of TUNEL positive cells compared with control (P<0.01) (**Figure 2C, 2D**). Meanwhile, Caspase-3 activity was increased dramatically after treatment by propofol, and the protein expression levels of NF-κB, bax and bcl-2 in A549 cells were all in accordance with the above (P<0.01) (**Figure 2E, 2F**).

Propofol increases rno-miR-665 and decreases bcl-xl expression in A549 cell

Rno-miR-665 was found to be expressed at elevated levels in A549 cells after 10 µM propofol treatment for 24 h (**Figure 3A**). Western blot analyses revealed that treatment of propofol significantly decreased the expression of bcl-xl in A549 cells (P<0.01) (**Figure 3B, 3C**).

Rno-miR-665 inhibits A549 cell proliferation

As shown in **Figure 4A**, rno-miR-665 expression was significantly upregulated after transfection with rno-miR-665 mimic in A549 cell,
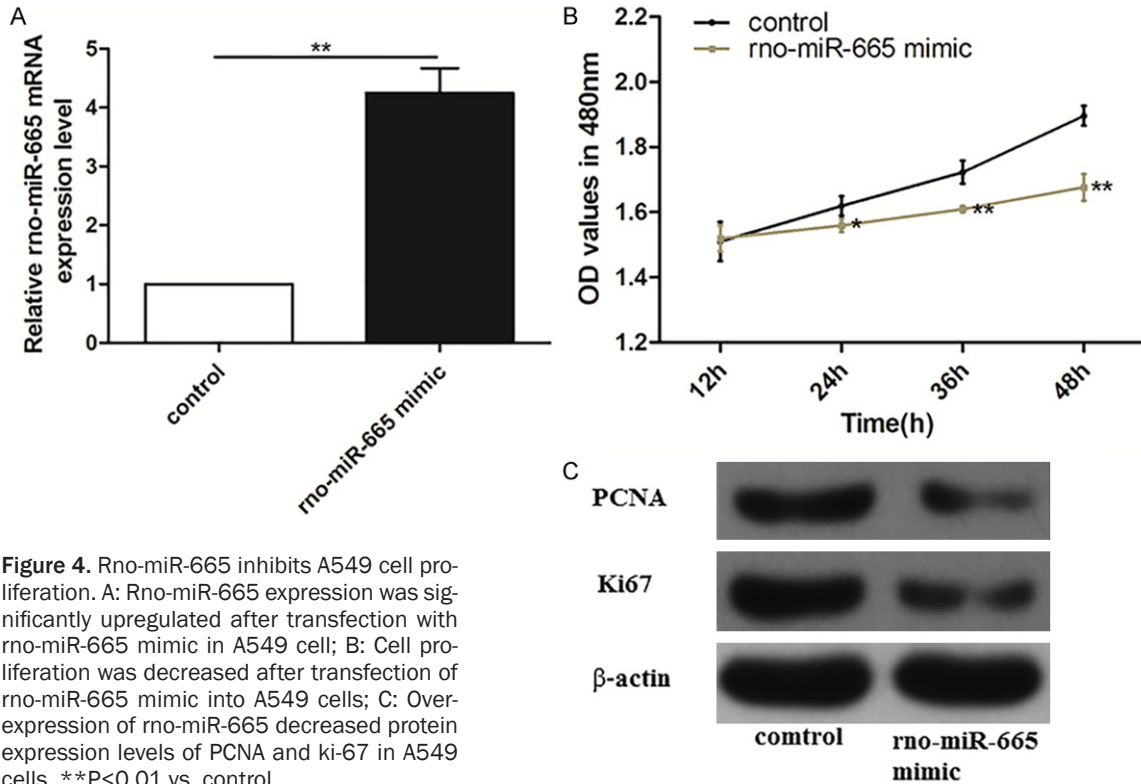
Figure 4. Rno-miR-665 inhibits A549 cell pro-
liferation. A: Rno-miR-665 expression was sig-
nificantly upregulated after transfection with
rno-miR-665 mimic in A549 cell; B: Cell pro-
liferation was decreased after transfection of
rno-miR-665 mimic into A549 cells; C: Over-
expression of rno-miR-665 decreased protein
expression levels of PCNA and ki-67 in A549
cells. **P<0.01 vs. control.

indicating that the mimic was efficiently trans-
fected (P<0.01). Transfection of rno-miR-665
mimic into A549 cells led to a decrease of cell
proliferation, and western blot examined that
overexpression of rno-miR-665 decreased pro-
tein expression levels of PCNA and ki-67 in
A549 cells (P<0.01) (**Figure 4B, 4C**).

*Rno-miR-665 induces cell apoptosis and de-
creases bcl-xl expression in A549 cell*

Pretreatment with rno-miR-665 mimic in A549
cell increased both early and late apoptotic cell
populations compared with the control (all pan-
els, P<0.01) (**Figure 5A, 5B**). Percentage of
TUNEL positive cells and caspase-3 activity in
A549 cell transfection with rno-miR-665 mimic
also significantly increased compared with con-
trol (all panels, P<0.01) (**Figure 5C-E**). In addi-
tion, expression levels of NF-κB and bax were
increased dramatically, while the protein of
bcl-2 and bcl-xl were all decreased significantly
in A549 cells (all panels, P<0.01) (**Figure 5F,
5G**).

*Rno-miR-665 inhibitor contributes to propofol
not alter proliferation of A549 cells*

As shown in **Figure 6A**, rno-miR-665 expres-
sion was significantly downregulated after

transfection with rno-miR-665 inhibitor in A549
cell, indicating that the inhibitor was efficiently
transfected (P<0.01). Propofol (1, 5 or 10 µM)
treatment for 48 h in A549 cell transfection
with rno-miR-665 inhibitor did not significantly
alter cell proliferation inhibition compared to
the control. We also found no changes in pro-
tein expression of PCNA and ki-67 in A549 cells
transfected with rno-miR-665 inhibitor (**Figure
6B, 6C**).

*Rno-miR-665 inhibitor contributes to propofol
not induce apoptosis of A549 cells*

Both early and late apoptotic cell populations in
flow cytometry and percentage of TUNEL posi-
tive cells in TUNEL assay were not altered sig-
nificantly when 10 µM propofol treatment for
24 h in A549 cells transfected with rno-
miR-665 inhibitor (**Figure 7A-D**). Meanwhile,
Caspase-3 activity and the protein expression
levels of NF-κB, bcl-2 and bax in A549 cells
transfected with rno-miR-665 inhibitor were
also not changing after treatment with propo-
fol, neither nor the expression of bcl-xl (**Figure
7E-G**).

Bcl-xl is a direct target of rno-miR-665

According to prediction of TargetScan and
miRanda database, we found that 3'-UTR of
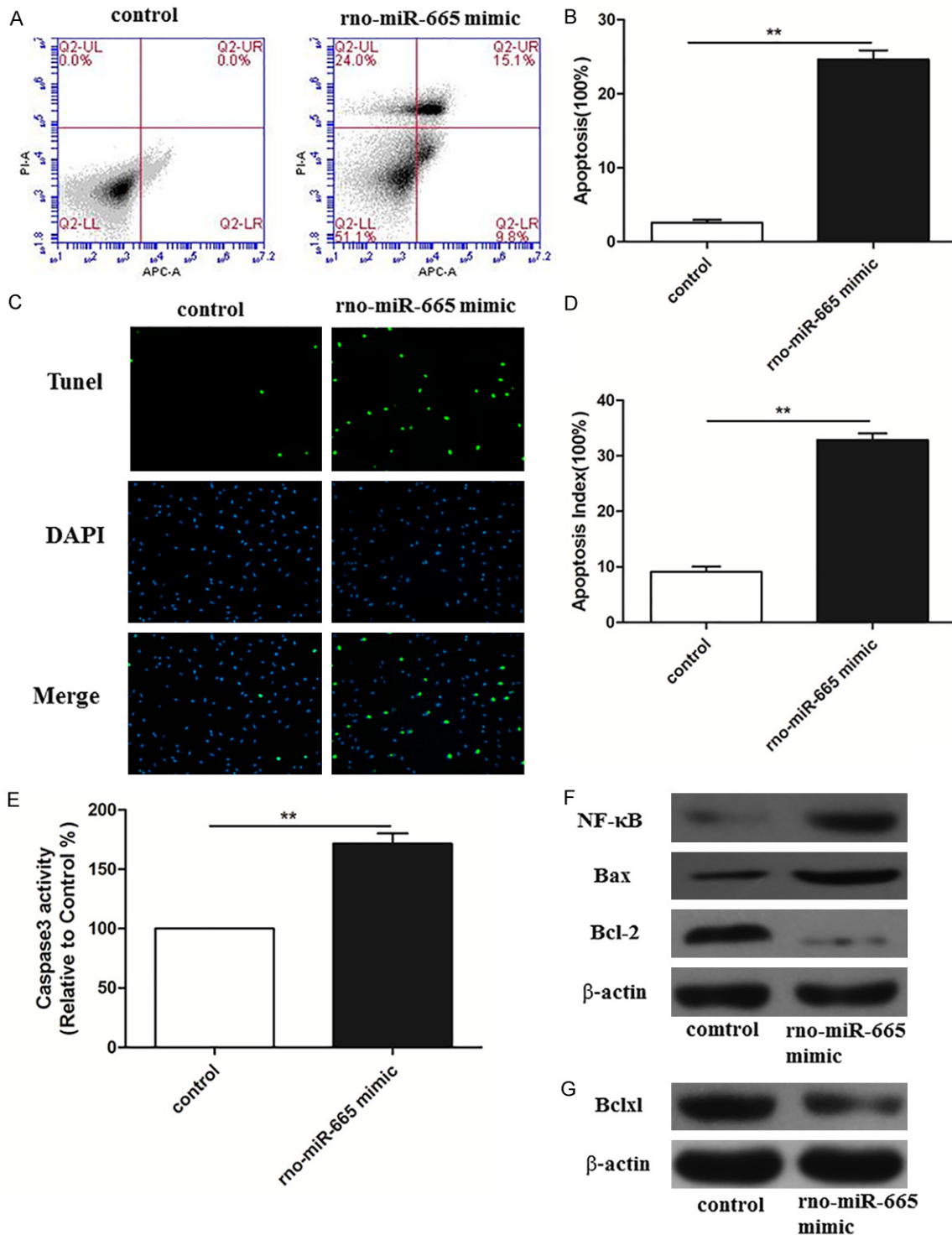
Figure 5. Rno-miR-665 induces cell apoptosis and decreases bcl-xl expression in A549 cells. A, B: Pretreatment with rno-miR-665 mimic in A549 cells increased both early and late apoptotic cell populations; C-E: Percentage of TUNEL positive cells and caspase-3 activity in A549 cell transfection with rno-miR-665 mimic also significantly increased compared with control; F, G: Expression levels of NF-κB and bax were increased dramatically, while the protein of bcl-2 and bcl-xl were all decreased significantly in A549 cells. **P<0.01 vs. control.

bcl-xl mRNA harbored a potential target site for rno-miR-665 (**Figure 8A**). Luciferase reporter

assay result showed that rno-miR-665 significantly suppressed the luciferase activity of the
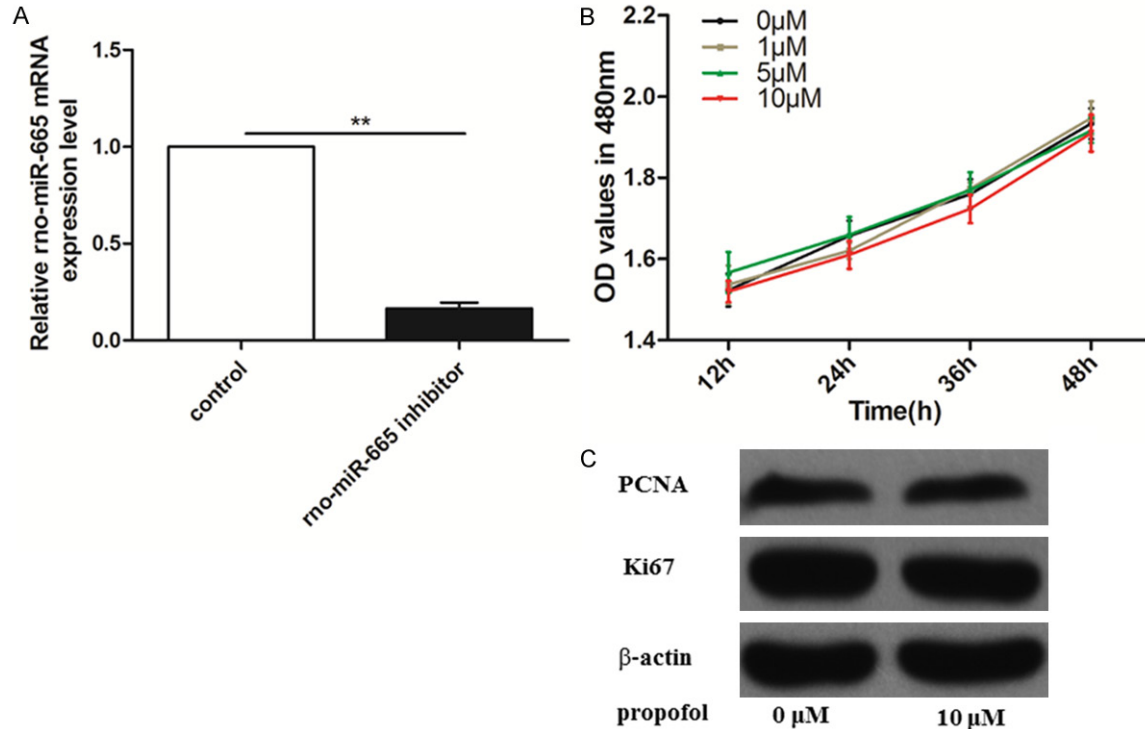
Figure 6. Rno-miR-665 inhibitor contributes to propofol not alter proliferation of A549 cells. A: rno-miR-665 expression was significantly downregulated after transfection with rno-miR-665 inhibitor in A549 cell; B: Different concentration of propofol (1, 5 or 10 μM) treated A549 cells transfection with rno-miR-665 inhibitor for 48 h did not significantly alter cell proliferation inhibition compared to the control; C: No changes in protein expression of PCNA and ki-67 in A549 cells transfected with rno-miR-665 inhibitor.

wild type (WT) rather than the mutant (MUT) 3'-UTR of bcl-xl (P<0.01) (**Figure 8B**). In addition to that over-expression of rno-miR-665 significantly decreased the expression of bcl-xl in A549 cells (P<0.01) (**Figure 5G**), our results suggest that bcl-xl might be a target of rno-miR-665 in A549 cells.

Discussion

In the present study, we assessed the roles of propofol on human lung cancer A549 cells and explored its mechanisms. We found that: 1) exposure to propofol inhibited proliferation and induced significant cell apoptosis in the A549 cells; 2) transfection with rno-miR-665 mimic in A549 cell inhibited cell proliferation and induced cell apoptosis; 3) transfection with rno-miR-665 inhibitor in A549 cells contributed to propofol not alter cell proliferation and apoptosis; 4) Bcl-xl was a direct target of rno-miR-665.

Propofol is an intravenous sedative-hypnotic agent administered to induce and maintain anesthesia. Its anticancer properties have been reported involve various mechanisms including direct and indirect suppression of the growth and proliferation of cancer cells by inducing apoptosis in some cancer cell lines [19-22]. Some in vitro evidence suggested that clinically relevant concentrations of propofol induced significant cell death in the hESC-derived neurons through regulation of miRNAs expression [23] and decreased the invasion ability of some human cancer cells [24, 25]. Liu et al found that propofol reduces cell death and leakage in a dose- and time-dependent manner in PANC-1 cells in vitro [20], which accords with our reports that propofol (1-10 μM) reduced cell proliferation in a dose- and time-dependent manner.

MiRNAs are endogenous small non-coding RNA molecules that regulate gene expression at the post-transcriptional level either by the promotion of mRNA degradation or by the inhibition of protein translation [26, 27]. For example, rno-miR-1224 and rno-miR-665 have been predict-
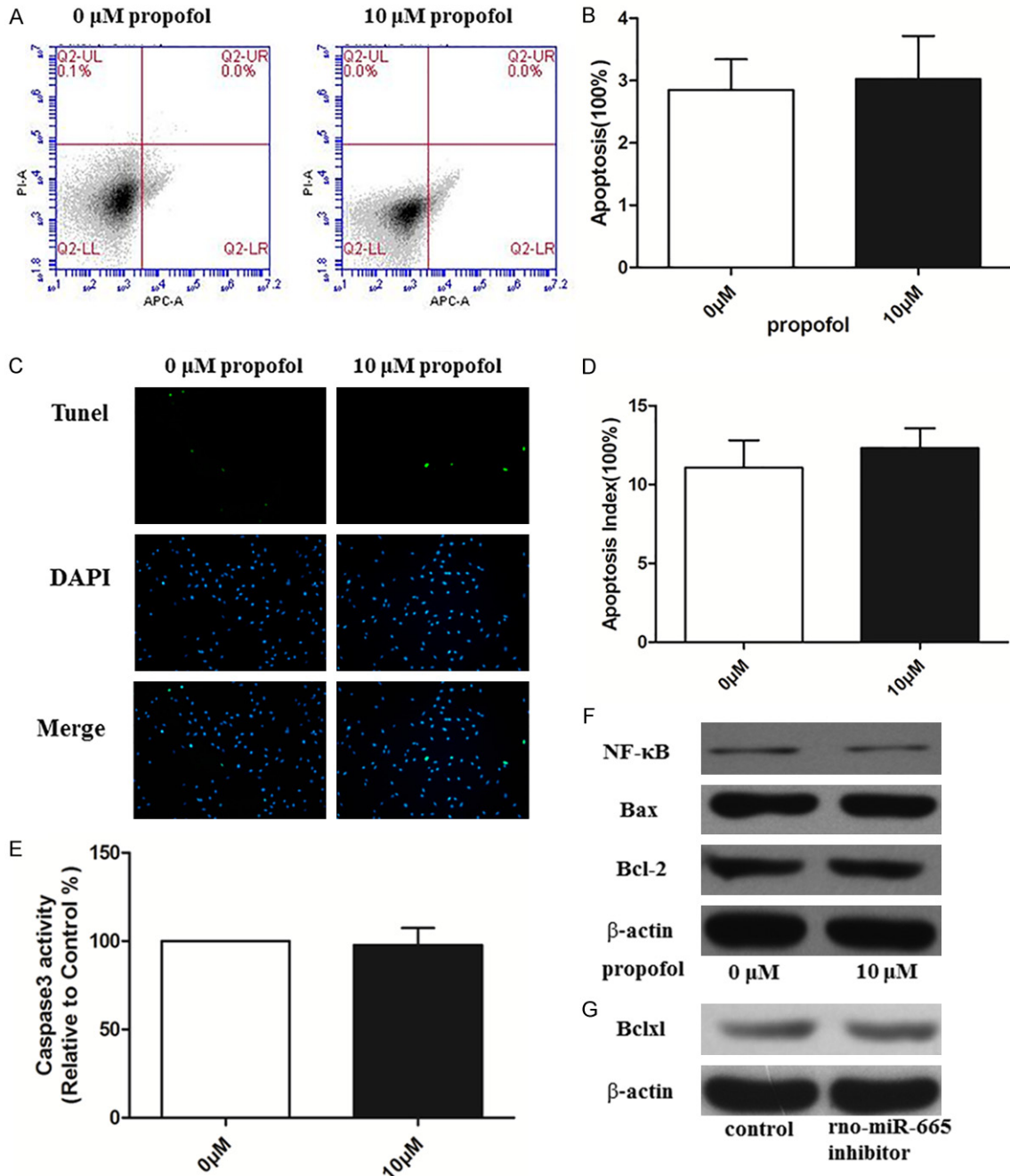
Figure 7. Rno-miR-665 inhibitor contributes to propofol not induce apoptosis of A549 cells. A-D: Both early and late apoptotic cell populations in flow cytometry and percentage of TUNEL positive cells in TUNEL assay were not altered significantly when 10 μM propofol treatment for 24 h in A549 cells transfected with rno-miR-665 inhibitor. E-G: Caspase-3 activity and the protein expression levels of NF-κB, bcl-2 and bax in A549 cells transfected with rno-miR-665 inhibitor were also not changing after treatment with propofol, neither nor the expression of bcl-xl.

ed to target Sox10 and Notch1 respectively, which control cell developmental processes. Similar to rno-miR-351-5p predicted to target Wnt11 and Tle3, which participate in the development and maintenance of the CNS. And com-

parable roles and Rno-miR-1224 targeted l1cam and Sox10 [12]. However, there has been a dearth of studies regarding regulation of propofol-mediated lung cancer suppression by miRNAs. Recently, Sun WC and Pei L report-
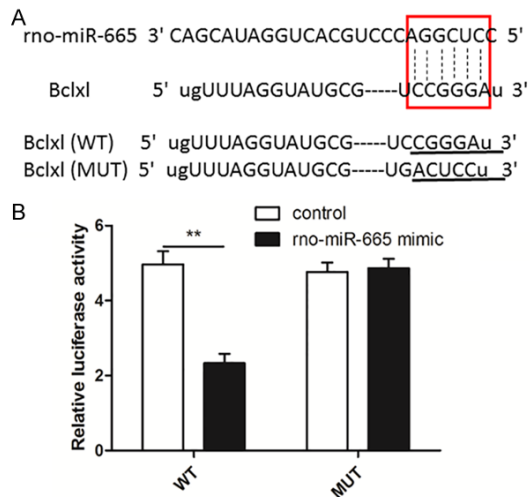
Figure 8. Bcl-xl is a direct target of rno-miR-665. A: 3'-UTR of bcl-xl mRNA harbored a potential target site for rno-miR-665; B: rno-miR-665 significantly suppressed the luciferase activity of the wild type (WT) rather than the mutant (MUT) 3'-UTR of Bcl-xl. **$P<0.01$ vs. control.

ed that rno-miR-665 targeted BCL2L1 (Bcl-xl) and increases vulnerability to propofol in developing astrocytes [28, 29], which accords with our research that rno-miR-665 mimic transfected in A549 cell inhibited cell proliferation and induced cell apoptosis, while transfection with rno-miR-665 inhibitor in A549 cells contributed to propofol not alter cell proliferation and apoptosis. Moreover, Bcl-xl was the direct target of rno-miR-665.

Conclusion

In summary, this study suggests that propofol inhibits proliferation and induces apoptosis of A549 cells through, at least partly, regulation of rno-miR-665. Although the clinical significance of our data remains to be verified in further studies, including animal trials and prospective clinical studies, our study provided a better understanding of propofol function in NSCLC cells.

Acknowledgements

Disclosure of conflict of interest

None.

Address correspondence to: Yingbin Wang, Department of Anesthesiology, The Second Hospital of Lanzhou University, 82 Cuiyingmen, Lanzhou 73-0030, Gansu Province, P. R. China. E-mail: wangyinbingslz@163.com

References

[1] Siegel R, Naishadham D and Jemal A. Cancer statistics, 2013. CA Cancer J Clin 2013; 63: 11-30.

[2] Russo A, Franchina T, Ricciardi GR, Picone A, Ferraro G, Zanghi M, Toscano G, Giordano A and Adamo V. A decade of EGFR inhibition in EGFR-mutated non small cell lung cancer (NSCLC): old successes and future perspectives. Oncotarget 2015; 6: 26814-26825.

[3] Goldstraw P, Crowley J, Chansky K, Giroux DJ, Groome PA, Rami-Porta R, Postmus PE, Rusch V, Sobin L; International Association for the Study of Lung Cancer International Staging Committee; Participating Institutions. The IASLC lung cancer staging project: proposals for the revision of the TNM stage groupings in the forthcoming (seventh) edition of the TNM Classification of malignant tumours. J Thorac Oncol 2007; 2: 706-714.

[4] Soon YY, Stockler MR, Askie LM and Boyer MJ. Duration of chemotherapy for advanced non-small-cell lung cancer: a systematic review and meta-analysis of randomized trials. J Clin Oncol 2009; 27: 3277-3283.

[5] Wang W, Lu R, Feng DY, Liang LR, Liu B and Zhang H. Inhibition of microglial activation contributes to propofol-induced protection against post-cardiac arrest brain injury in rats. J Neurochem 2015; 134: 892-903.

[6] Tao T, Li CL, Yang WC, Zeng XZ, Song CY, Yue ZY, Dong H and Qian H. Protective effects of propofol against whole cerebral ischemia/reperfusion injury in rats through the inhibition of the apoptosis-inducing factor pathway. Brain Res 2016; 1644: 9-14.

[7] Liu F, Chen MR, Liu J, Zou Y, Wang TY, Zuo YX and Wang TH. Propofol administration improves neurological function associated with inhibition of pro-inflammatory cytokines in adult rats after traumatic brain injury. Neuropeptides 2016; 58: 1-6.

[8] Wigmore TJ, Mohammed K and Jhanji S. Long-term survival for patients undergoing volatile versus IV anesthesia for cancer surgery: a retrospective analysis. Anesthesiology 2016; 124: 69-79.

[9] Labelle M and Hynes RO. The initial hours of metastasis: the importance of cooperative host-tumor cell interactions during hematogenous dissemination. Cancer Discov 2012; 2: 1091-1099.

[10] Christopherson R, James KE, Tableman M, Marshall P and Johnson FE. Long-term survival after colon cancer surgery: a variation associated with choice of anesthesia. Anesth Analg 2008; 107: 325-332.

[11] Biki B, Mascha E, Moriarty DC, Fitzpatrick JM, Sessler DI and Buggy DJ. Anesthetic technique for radical prostatectomy surgery affects cancer recurrence: a retrospective analysis. Anesthesiology 2008; 109: 180-187.

[12] Sun W and Pei L. MicroRNA expression profiling of propofol-treated developing rat hippocampal astrocytes. DNA Cell Biol 2015; 34: 511-523.

[13] Guo H, Ingolia NT, Weissman JS and Bartel DP. Mammalian microRNAs predominantly act to decrease target mRNA levels. Nature 2010; 466: 835-840.

[14] Bartel DP. MicroRNAs: target recognition and regulatory functions. Cell 2009; 136: 215-233.

[15] Faversani A, Amatori S, Augello C, Colombo F, Porretti L, Fanelli M, Ferrero S, Palleschi A, Pelicci PG, Belloni E, Ercoli G, Degrassi A, Baccarin M, Altieri DC, Vaira V and Bosari S. MiR-494-3p is a novel tumor driver of lung carcinogenesis. Oncotarget 2017; 8: 7231-7247.

[16] Zhang J, Fu J, Pan Y, Zhang X and Shen L. Silencing of miR-1247 by DNA methylation promoted non-small-cell lung cancer cell invasion and migration by effects of STMN1. Onco Targets Ther 2016; 9: 7297-7307.

[17] Liu W, Xiao P, Wu H, Wang L, Kong D and Yu F. MicroRNA-98 plays a suppressive role in non-small cell lung cancer through inhibition of SALL4 protein expression. Oncol Res 2016; [Epub ahead of print].

[18] Kyrylkova K, Kyryachenko S, Leid M and Kioussi C. Detection of apoptosis by TUNEL assay. Methods Mol Biol 2012; 887: 41-47.

[19] Huang H, Benzonana LL, Zhao H, Watts HR, Perry NJ, Bevan C, Brown R and Ma D. Prostate cancer cell malignancy via modulation of HIF-1alpha pathway with isoflurane and propofol alone and in combination. Br J Cancer 2014; 111: 1338-1349.

[20] Liu Z, Zhang J, Hong G, Quan J, Zhang L and Yu M. Propofol inhibits growth and invasion of pancreatic cancer cells through regulation of the miR-21/Slug signaling pathway. Am J Transl Res 2016; 8: 4120-4133.

[21] Huang X, Teng Y, Yang H and Ma J. Propofol inhibits invasion and growth of ovarian cancer cells via regulating miR-9/NF-kappaB signal. Braz J Med Biol Res 2016; 49: e5717.

[22] Twaroski DM, Yan Y, Olson JM, Bosnjak ZJ and Bai X. Down-regulation of microRNA-21 is involved in the propofol-induced neurotoxicity observed in human stem cell-derived neurons. Anesthesiology 2014; 121: 786-800.

[23] Vorvis C, Koutsioumpa M and Iliopoulos D. Developments in miRNA gene signaling pathways in pancreatic cancer. Future Oncol 2016; 12: 1135-1150.

[24] Mammoto T, Mukai M, Mammoto A, Yamanaka Y, Hayashi Y, Mashimo T, Kishi Y and Nakamura H. Intravenous anesthetic, propofol inhibits invasion of cancer cells. Cancer Lett 2002; 184: 165-170.

[25] Miao Y, Zhang Y, Wan H, Chen L and Wang F. GABA-receptor agonist, propofol inhibits invasion of colon carcinoma cells. Biomed Pharmacother 2010; 64: 583-588.

[26] Hou J, Meng F, Chan LW, Cho WC and Wong SC. Circulating plasma MicroRNAs as diagnostic markers for NSCLC. Front Genet 2016; 7: 193.

[27] Hernandez L, Hsu SC, Davidson B, Birrer MJ, Kohn EC and Annunziata CM. Activation of NF-kappaB signaling by inhibitor of NF-kappaB kinase beta increases aggressiveness of ovarian cancer. Cancer Res 2010; 70: 4005-4014.

[28] Sun WC and Pei L. Rno-miR-665 targets BCL2L1 (Bcl-xl) and increases vulnerability to propofol in developing astrocytes. J Neurochem 2016; 138: 233-242.

[29] Sun WC, Liang ZD and Pei L. Propofol-induced rno-miR-665 targets BCL2L1 and influences apoptosis in rodent developing hippocampal astrocytes. Neurotoxicology 2015; 51: 87-95.